Ultrasonic measurements of an epoxy resin near its sol-gel transition

D. L. Sidebottom*
Department of Material Science and Engineering, McMaster University, Hamilton, Ontario, Canada L8S 4L7
(Received 17 June 1992; revised manuscript received 16 February 1993)

Measurements of the change in attenuation and transit time of high-frequency (5 MHz) longitudinal sound waves through an epoxy resin as it proceeds through the sol-gel transition are presented. The transition from viscoelastic liquid to elastic solid results from the formation of permanent cross-links and is well suited to an interpretation in terms of percolation concepts. At high frequency, the exponents k and t, which describe the critical behavior of the viscosity and elasticity, respectively, are modified considerably as compared with corresponding static values, but in a manner consistent with extensions of percolation theory to the high-frequency regime. Interestingly, it is observed that at high frequency, "dangling chains" appear to contribute to the elasticity, resulting in the exponent t approaching β, that of the gel fraction.

PACS number(s): 82.70.Gg, 61.41.+e, 62.90.+k, 05.20.−y

INTRODUCTION

The general features of the gelation transition that occurs in many natural and man-made materials are presently well understood. They are the result of random bond formation in a liquid solution (sol) which leads eventually to a highly cross-linked elastic network (gel) which permeates the material [1,2]. Early works by Flory [3] and Stockmayer [4], and later by de Gennes [5] and Stauffer [6], have been successful in qualitatively explaining many of the features of such random bond-formation processes. These theoretical approaches are broadly referred to as percolation theory (PT) [7] and have evolved to describe the connectivity properties of randomly forming bonds on a D-dimensional lattice. PT predicts that upon increasing the fraction of bonds p, clusters of bonded material develop until at the percolation threshold p_c a specific cluster exists which effectively spans the entire lattice. The transition from finite to infinite is rapid and the connectivity length, a measure of the mean cluster size, diverges as a power law of the form $\xi=\xi_0\Delta p^{-\nu}$, where $\Delta p=|p-p_c|/p_c$. Beyond p_c, smaller clusters become incorporated into the infinite cluster and its mass increases rapidly. The probability that a bond belongs to the infinite cluster (the gel fraction) vanishes on approach to p_c from above as $S_\infty=\Delta p^{\beta}$. The problem of bonds forming randomly on a lattice has been extensively studied by computer simulations and the exponents that characterize these divergences are well known. In three dimensions, $\nu=0.88$ and $\beta=0.45$.

Physically, gels are classified into two extreme situations [1,8]. Weak (reversible) gels are gels in which the fraction of bonds can be controlled by variation of one or more thermodynamic fields, such as temperature. A common example of a weak gel is the gelatin-water system which is often found in many work place cafeterias. Here the bonds form due to suppression of the temperature and can be destroyed by subtle warming. As the bonds are reversible, the threshold is not sharply defined and the transition from viscous liquid to elastic matter often exhibits frequency-dependent properties similar to those seen in glass transitions. Further, weak gels are often produced in the presence of a solvent which can contribute to the dynamics. At the other extreme are strong (irreversible) gels. Strong gels, such as epoxy resins, form cross-links via a chemical reaction. The cross-links so formed are permanent and stable against changes in thermodynamic fields. This irreversibility sharpens the threshold resulting in a transition more nearly like that of the percolation model.

The behavior of transport properties such as the viscosity η and elastic modulus G' of substances in the vicinity of the gelation threshold has been widely discussed [9–11]. Experimentally one finds that rapid variations occur in the transport properties on approach to p_c. The viscosity diverges as a power law below p_c, as

$$\eta\approx\Delta p^{-k}\,, \tag{1}$$

while the elastic modulus vanishes on approach to p_c from above as

$$G'\approx\Delta p^{t}\,. \tag{2}$$

The power-law nature of these quantities naturally suggests an underlying connection to PT. However, it is important to stress that PT considers only the connectivity properties and thus represents only the static nature of the bonded network. It cannot by itself describe the dynamic behavior associated with transport quantities such as η and G' discussed above. Instead, use is commonly made of an analogy first proposed by de Gennes [5] that the transport properties should behave in the same way as the conductivity of a percolating network of conducting elements. For the sol phase ($p<p_c$) the viscosity is thought to behave like the conductivity of a mixture of superconductors and resistors, while for the gel phase, the elastic modulus follows the conductivity of a mixture of resistors and insulators. These models reproduce the power-law features of Eqs. (1) and (2), respectively.

Although some have questioned the validity of de

Gennes analogy [9,12], it is nevertheless an attractive approach as it allows one to bridge the gap between PT and transport properties without needing to consider microscopic details regarding the elastic nature of the bonds.

Present estimates from computer simulation for the dc conductivity give $k=k_0=0.7$ and $t=t_0=2$ in three dimensions. The subscripts indicate exponents for the zero-frequency case. Experimentally, these zero-frequency exponents scatter with k_0 ranging from 0.7 to 1.5 and t_0 ranging from 2 to 3.8 [9]. The exponent t_0 is generally larger than that of the gel fraction β due to the existence of dangling chains [1]. These are polymer segments which are free at one end. Although they contribute to the mass of the infinite cluster, they do not contribute to the elasticity in the zero-frequency situation.

However, measurements of η and G' are often performed at some finite frequency and the exponents may be modified considerably from those found in the static situation above ($k_0=1.1\pm0.4$ and $t_0=2.9\pm0.9$). How these exponents are modified is the subject of the next section, where a description of the dependence of both η and G' upon frequency around the gel point is developed using simple concepts taken from viscoelastic theory.

THEORY

In a viscoelastic medium, the complex shear modulus G^*, consists of both an elastic contribution (storage) which is in phase with the applied stress as well as a viscous contribution (loss) which is 90° out of phase, such that

$$G^*(\omega)=G'(\omega)+i\omega\eta(\omega) . \tag{3}$$

This division of G^* into elastic and viscous components is illustrated in the following simple model first proposed by Maxwell. In the Maxwell model, a viscoelastic element is represented by a spring, with spring constant G', connected in series with a dashpot whose drag coefficient is η. The response of this element to an applied oscillatory stress results in two distinct behaviors depending upon the frequency.

In the limit of low frequency, applied stress results mostly in the dissipation of energy into heat due to viscous flow in the dashpot. Thus

$$\lim_{\omega\to 0}|G^*|=\omega\eta_0 , \tag{4}$$

where η_0 is the zero-frequency viscosity.

At high frequency, applied stress is mostly stored as elastic energy in the spring. Hence

$$\lim_{\omega\to\infty}|G^*|=G_\infty , \tag{5}$$

where G_∞ is the infinite-frequency elasticity.

Between these two limits the frequency dependence of G^* is described by a response function of the form

$$G^*=G_\infty\frac{\omega^2/\omega_c^2+i\omega/\omega_c}{1+\omega^2/\omega_c^2} , \tag{6}$$

where ω_c is the Maxwell frequency defined as

$$\omega_c=\frac{G_\infty}{\eta_0} . \tag{7}$$

Although this specific response function is special to the Maxwell model, a review of most any standard text on the subject of linear viscoelasticity [13] reveals that G^* is quite commonly controlled by a single characteristic frequency scale. Since only one relevant frequency scale is present, this implies that G^* exhibits scaling properties and can be expressed most generally in terms of the reduced variable ω/ω_c such that

$$G^*(i\omega)=G_\infty\phi(i\omega/\omega_c) . \tag{8}$$

One sees that the response function of the Maxwell model given in Eq. (6) is consistent with the general scaling form given by Eq. (8).

In the case of supercooled liquids, for example, the real and imaginary parts of G^* commonly exhibit response functions which, although they depend strongly upon temperature, are found to collapse about a common curve once the frequency is scaled by a temperature-dependent characteristic frequency. This characteristic frequency is again given by Eq. (7), but for simple glass-forming liquids, G_∞ remains relatively temperature insensitive while η_0 grows rapidly upon cooling into the glassy state. This leads to a characteristic frequency which varies inversely to η_0 and vanishes near the glass transition.

For the sol-gel transition, however, ω_c evolves under isothermal conditions due to the formation of clusters leading to an extensively bonded network. Thus changes in ω_c result from changes in both η_0 and G_∞. In order to develop a scaling approach for the sol-gel transition, an appropriate form for the scaling function $\phi(z)$ must be devised which produces the experimentally witnessed power-law behaviors of both η and G'. Since these two quantities display contrasting behavior (η diverges while G' vanishes) on approach to p_c, it is common [14,15] to construct $\phi(z)$ in a piecewise fashion such that Eq. (8) is generalized as

$$\omega\eta=G_-=G_\infty\phi_-(\omega/\omega_c) , \quad p<p_c , \tag{9a}$$

$$G'=G_+=G_\infty\phi_+(\omega/\omega_c) , \quad p>p_c , \tag{9b}$$

and the two scaling functions constrained to agree at $p=p_c$. From Eqs. (9a) and (9b) this constraint implies

$$\omega\eta\approx G' , \quad p=p_c . \tag{9c}$$

Again, since η and G' exhibit opposing power-law dependences away from p_c, in order to satisfy Eq. (9c) both must eventually cross over from their respective power laws and approach p_c in a Δp-independent manner [14],

$$\omega\eta\approx G'\approx\Delta p^0 , \quad p\approx p_c . \tag{10}$$

Response functions for η and G' for the sol-gel situation can now be developed. The characteristic frequency is again given by Eq. (7), where the zero-frequency divergence of the viscosity is generalized from Eq. (1) as

$$\eta_0=\eta_0^0\Delta p^{-k_0} ,$$

where $\eta_0^0=\eta_0(p=0)$, and the infinite frequency elasticity is generalized from Eq. (2) as

$$G_\infty = G_\infty^1 \Delta p^{t_\infty} ,$$

where $G_\infty^1 = G_\infty(p=1)$. The characteristic frequency vanishes on approach to p_c as

$$\omega_c = \frac{G_\infty}{\eta_0} = \frac{G_\infty^1 \Delta p^{t_\infty}}{\eta_0^0 \Delta p^{-k_0}} = \omega_0 \Delta p^{k_0+t_\infty} , \tag{11}$$

where t_∞ is the infinite frequency value of t, and k_0 is the zero-frequency value of k. Thus, from Eqs. (9a) and (9b),

$$G_\pm(\omega) = G_\infty \phi_\pm(\omega/\omega_c) = G_\infty^1 \Delta p^{t_\infty} \phi_\pm \left[\frac{\omega}{\omega_0} \Delta p^{-k_0-t_\infty} \right] . \tag{12}$$

The piecewise scaling function

$$\phi_-(z) = az + bz^2 + \cdots , \quad p < p_c , \tag{13a}$$

$$\phi_+(z) = 1 + cz^{-1} + \cdots , \quad p > p_c , \tag{13b}$$

$$\phi_\pm(z) = z^u , \quad p \approx p_c \tag{13c}$$

is proposed and shown below to yield the appropriate behavior when the limits in both ω and Δp outlined above [see Eqs. (1), (2), (4), (5), and (10)] are applied.

For $p < p_c$, Eqs. (12) and (9a) together with Eq. (13a) result in

$$\eta = \frac{G_-}{\omega} = \frac{G_\infty^1 \Delta p^{t_\infty}}{\omega} \left[a \left[\frac{\omega}{\omega_0} \right] \Delta p^{-k_0-t_\infty} + b \left[\frac{\omega}{\omega_0} \right]^2 \Delta p^{-2k_0-2t_\infty} + \cdots \right] . \tag{14}$$

In the zero-frequency limit, higher-order terms in ω vanish, leaving

$$\eta_0 = \eta_0^0 \Delta p^{-k_0} . \tag{15a}$$

However, as ω increases, far from p_c, the next higher order in ω eventually dominates, leading to

$$\eta = \eta_0^0 \left[\frac{\omega}{\omega_0} \right] \Delta p^{-k_\infty} , \tag{15b}$$

where k_∞ is defined by

$$k_\infty = 2k_0 + t_\infty . \tag{15c}$$

For $p > p_c$, Eqs. (12) and (9b) together with Eq. (13b) result in

$$G' = G_+ = G_\infty^1 \Delta p^{t_\infty} \left[1 + c \left[\frac{\omega}{\omega_0} \right]^{-1} \Delta p^{k_0+t_\infty} + \cdots \right] . \tag{16}$$

In the limit of infinite frequency, higher-order terms again vanish, leaving

$$G_\infty = G_\infty^1 \Delta p^{t_\infty} . \tag{17a}$$

However, as ω decreases, far from p_c, the second term dominates such that

$$G' = G_\infty^1 \left[\frac{\omega}{\omega_0} \right]^{-1} \Delta p^{t_0} , \tag{17b}$$

where t_0 is defined by

$$t_0 = k_0 + 2t_\infty . \tag{17c}$$

Sufficiently close to p_c, the power laws of both η and G' cross over toward a behavior independent of Δp. This crossover is suggested by others [14] to occur when $\omega \approx \omega_c$. At $p = p_c$, Eq. (9c), together with Eqs. (12) and (13c), becomes

$$\omega\eta \approx G' = G_\infty^1 \Delta p^{t_\infty} \left[\frac{\omega}{\omega_0} \Delta p^{-k_0-t_\infty} \right]^u = G_\infty^1 \left[\frac{\omega}{\omega_0} \right]^u \Delta p^{t_\infty - u(k_0+t_\infty)} . \tag{18}$$

Again, since both η and G' must approach p_c in a Δp-independent fashion, Eq. (10) then constrains the exponent u, such that

$$t_\infty - u(k_0 + t_\infty) = 0$$

or

$$k_0 = t_\infty \left[\frac{1}{u} - 1 \right] . \tag{19}$$

Thus one finds from Eq. (18) that at $p = p_c$, both η and G' exhibit an anomalous power law dispersion in ω such that

$$\eta \approx \omega^{u-1} , \tag{20a}$$

$$G' \approx \omega^u . \tag{20b}$$

Comparison with the literature [10,14,15] indicates that the results of the above derivation are in many ways similar to those of the scaling hypothesis approach, first introduced by Efros and Shklovskii (ES) [15]. However, the simpler approach presented here has resulted in one key difference. In the present work, consideration of the limiting behavior of a simple viscoelastic element has quite naturally lead to the construction of a scaling function for G' based upon an infinite-frequency-limit strategy. ES and others establish the scaling ansatz in terms of a zero-frequency limit of G'. The zero-frequency approach of ES requires Eq. (12) to take the form

$$G_\pm^{\mathrm{ES}}(\omega) = G_0^1 \Delta p^{t_0} \phi_\pm \left[\frac{\omega}{\omega_0'} \Delta p^{-k_0-t_0} \right] , \tag{21}$$

with the scaling relation Eq. (13b) recast as

$$\phi_+^{\mathrm{ES}}(z) = 1 + cz + \cdots , \tag{22}$$

such that additional terms are truncated at zero frequency. Furthermore, the ES approach results in the fundamental scaling relation, Eq. (19), being replaced by

$$k_0 = t_0 \left[\frac{1}{u} - 1 \right], \quad (\mathrm{ES}) . \tag{23}$$

Although appropriate for describing features of the low-frequency behavior of η and G', it is shown later that the alternative scaling function implied by the zero-frequency approach of ES [Eq. (22)] poses problems in the high-frequency situation.

To summarize, the above derivation results in the following predicted behavior.

In the low-frequency limit,

$$\eta \approx \Delta p^{-k_0}, \quad k_0 = t_\infty \left[\frac{1}{u} - 1 \right], \quad p < p_c \tag{24a}$$

$$G' \approx \Delta p^{t_0}, \quad t_0 = t_\infty \left[\frac{1}{u} + 1 \right], \quad p > p_c . \tag{24b}$$

In the high-frequency limit,

$$\eta \approx \Delta p^{-k_\infty}, \quad k_\infty = t_\infty \left[\frac{2}{u} - 1 \right], \quad p < p_c , \tag{25a}$$

$$G' \approx \Delta p^{t_\infty}, \quad p > p_c . \tag{25b}$$

Near p_c,

$$\eta \approx \Delta p^0 \omega^{u-1} , \tag{26a}$$

$$G' \approx \Delta p^0 \omega^u , \tag{26b}$$

and the crossover from the power-law behavior in Δp to power-law dispersion in ω is governed by the condition

$$\omega/\omega_c = 1 \quad \text{or} \quad \omega \left[\frac{\eta_0^0}{G_\infty^1} \right] = \Delta p^{k_0 + t_\infty} . \tag{27}$$

In this paper, ultrasonic measurements (2–10 MHz) of changes in the attenuation and velocity of sound in an epoxy resin as it proceeds through the gel transition are presented. These quantities are directly related to η and G', respectively, and are shown to display appropriate power-law divergences on approach to the percolation threshold as well as the appropriate dispersion at the threshold. The measured exponents (k, t, and u) are found to differ significantly from those commonly seen in the literature. This finding only underscores the importance of the frequency dependencies of these exponents. Instead it is shown that the measured exponents are consistent with the formalism outlined above.

METHOD

Measurements of the change in attenuation and the change in transit time of a longitudinal-acoustic-wave pulse were performed at selected time intervals during the cure of an epoxy resin. The epoxy chosen for this study was diglycidyl ether of bisphenol-A (DGEBA) marketed by Shell under the trade name Epon 815. The curing agent was triethylenetetramine (TETA), supplied by Aldrich Chemicals. This particular system was selected for its quickness of preparation as both parts are liquid at room temperature and can be easily mixed. DGEBA has a functionality of 2 and TETA a functionality of 6 and in all cases stoichiometric mixtures to give approximately 8 ml volume were prepared from the reagents just prior to measurement. For measurements above ambient temperature, the separate elements were preheated to the desired curing temperature before mixing to best achieve isothermal conditions over the entire duration of cure. The mixing was done manually and usually completed within about 30 s. Immediately after mixing, the sample was transferred into a preheated ultrasonic cell.

The ultrasonic cell consisted of an aluminum cylinder (1 in. i.d.) into which was tightly fitted a commercially available (Harisonics) transducer at one end (receiver) and a 4.5-cm aluminum buffer rod at the other end terminated by a second transducer (transmitter). The second transducer was contacted to the far end of the buffer rod by a thin layer of Dow Corning vacuum grease and aligned by a tight-fitting brass sleeve. The length of the buffer rod was chosen to ensure that the wave propagating in the sample was in the far-field domain of the pressure interference pattern that is created by the finite size (0.75 in. diam.) of the ultrasonic source.

The sample was pipetted into the cell through a hole located at the top and great care was exercised to avoid the formation of bubbles. The sample filled a section of the cylinder terminated by 0.66-cm-thick walls made of Plexiglas. Plexiglas walls maintained good acoustical coupling to the sample and allowed the final sample to be removed and the cell reused. The exterior of these walls and the transducer on one side and the transducer with buffer rod on the other were acoustically bonded with a thin layer of vacuum grease. Measurements at 2.25 MHz were performed using a 0.65-cm path length, while measurements at 5 and 10 MHz required a shorter (0.15 cm) path length.

The entire cell, buffer rod, and transducers were held in a clamping device and placed inside a regulated oven (± 2 K). The temperature was determined from measurement of a thermocouple which was placed in contact with the sample but not in the path of the ultrasonic beam. All these precautions were, however, unable to avoid a drift of about 5 K during the initial stages (≈ 300 s) which arose from the exothermic nature of the chemical reaction.

Measurements of the change in intensity of the received pulse relative to a fixed reference and changes in the transit time of this pulse were acquired automatically at selected time intervals using a commercially available ultrasonic system (Matec MBS-8000) interfaced to a small computer. This system employs a phase-detection technique of which a description can be found in the literature [16].

Measurement of the absolute attenuation was not attempted as it is considerably influenced by losses which occur at the interfaces. A value of the absolute velocity at the start of cure was obtained with an uncertainty of $\pm 10\%$. Relative changes in the attenuation and transit time, however, are accurate to about $\pm 1\%$.

The propagation of longitudinal acoustic waves in a viscoelastic medium is described by the speed of propagation v and attenuation α. These properties are related to

the complex longitudinal modulus $M^*=M'+iM''$ as

$$\rho v^2=M'=K'+\tfrac{4}{3}G' , \tag{28}$$

$$\frac{2\rho\alpha v^3}{\omega^2}=\frac{M''}{\omega}=\zeta+\tfrac{4}{3}\eta , \tag{29}$$

where ρ is the density, K' is the volume (bulk) modulus, G' is the shear modulus, ζ is volume (bulk) viscosity, and $\eta=G''/\omega$ is the shear viscosity.

As changes in the density throughout the transition are typically less than 5%, ρ is regarded as a constant. Furthermore, for the transition from liquid to an elastic solid via chemical cross-linking, one anticipates that the dominant contribution to changes in M^* arises from changes in the shear terms and thus the bulk terms are assumed to be sufficiently constant. Finally, the usual assumption is made that sufficiently close to p_c the rate of bond formation is constant and that $t-t_g=p-p_c$, where t_g is the gelation time at which $p=p_c$. Under these assumptions one obtains

$$\Delta v^2\approx G'\approx\Delta t^t , \tag{30}$$

$$\Delta(\alpha v^3)\approx\eta\approx\Delta t^{-k} , \tag{31}$$

where $\Delta t=|t-t_g|/t_g$. The velocity is related to the measured initial transit time τ_0 and decreases in transit time $\Delta\tau$ as

$$v^{-1}=\frac{\tau_0}{d}-\frac{\Delta\tau}{d} ,$$

where d is the path length through the sample.

RESULTS

Measurements of $\Delta\alpha$ and the decrease in transit time per unit length $\Delta\tau/d$ are shown for four curing temperatures T_c from 55 °C to 8 °C in Figs. 1(a) and 1(b), respectively. One recognizes immediately a pronounced peak in the attenuation occurs some period of time after mixing. The decrease in transit time (roughly the increase in the velocity) increases monotonically and at roughly the same time exhibits a point of inflection. The time interval at which these rapid changes occur and the width of the transition region increases with decreasing temperature due to the higher viscosity of the initial sol, which results in slower diffusion and hence a slower rate of bond formation.

Such behavior is reminiscent of relaxation processes and some [17] have also interpreted it as such. Although there certainly exist relaxation processes which contribute to the attenuation, it is believed that the dominant contribution will come from the macroscopic changes in the viscosity which diverges on approach to t_g. It is noted that for DGEBA in the temperature range investigated (size $\approx$30 Å, $\eta>0.1$ Pa s) the rotational relaxation frequency is of the order of 100 kHz or less and lies well below the probe frequency of these measurements. Other relaxation processes often witnessed in glasses and attributed to localized motions of the polymer (so-called β relaxations) [18] may also contribute beyond t_g; however, these are typically much weaker processes.

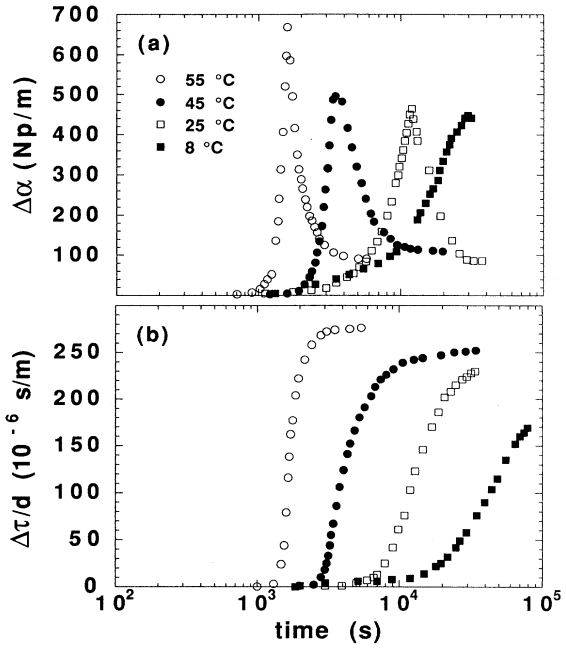

FIG. 1. (a) Change in attenuation vs. curing time at $\nu=2.25$ MHz for $T=55$ °C–8 °C. (b) Decrease in transit time per unit length vs. curing time for $T=55$ °C–8 °C.

The rise of the attenuation is analyzed in terms of Eq. (31) by plotting $\Delta\alpha v^3$ vs. Δt in a double logarithmic plot (Fig. 2). For lack of any better criterion, t_g is defined as the time where $\Delta\alpha$ reaches a maximum. In Fig. 2, one observes evidence of a power-law behavior with k $(=k_\infty)=4\pm0.5$ far from the gel point. As Δt approaches zero, this power law breaks down and $\Delta\alpha v^3$ approaches a constant independent of Δt, as expected when the system crosses over into the dispersion regime near t_g.

The growth of the elastic modulus is depicted in Fig. 3 by the variation of Δv^2. Near the gel point, the data display power-law behavior with a temperature-independent exponent $t(=t_\infty)=0.47\pm0.03$. As time in-

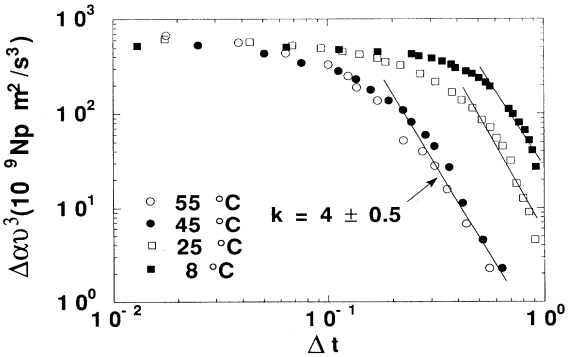

FIG. 2. Plot of $\Delta\alpha v^3$ vs. Δt at $\nu=2.25$ MHz for $T=55$ °C–8 °C. The lines represent fits of Eq. (31) at large Δt with $k=4.0\pm0.5$.

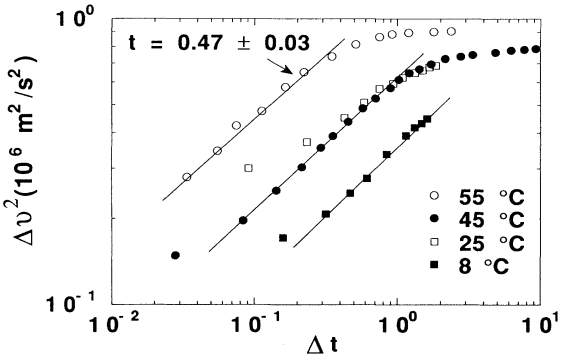

FIG. 3. Plot of Δv^2 vs. Δt for 55 °C–8 °C. The lines represent fits of Eq. (30) with $t=0.47\pm0.03$.

creases far beyond t_g, the power law breaks down. This is simply a consequence of the eventual failure in the assumed linear relationship between time and bond formation. Time continues without limit, but the number of possible bonds is finite.

As an additional test the decrease of $\Delta\alpha$ that occurs after t_g is considered. In Fig. 4 one finds that over an intermediate range, $\Delta\alpha$ follows a power law with an exponent of about -0.65 ± 0.03. This decrease in attenuation is presumably a direct result of the increasing elasticity of the medium which affects an improved transmission of sound. Assuming that the loss G'', as expected for an anharmonic elastic medium, approaches some constant limit beyond t_g, Eq. (31) indicates that $\Delta\alpha\approx v^{-3}$ or that $\Delta\alpha\approx\Delta t^{-(3/2)t}$ from which one again obtains $t\ (=t_\infty)=0.44\pm0.03$.

It is important at this point to also stress the difference in the behavior of the attenuation of the epoxy system studied here which contains no solvent with that of the gelatin-water system studied by Bacri *et al.* [19], for which the solvent (water) plays a dominant role. They observed an attenuation that remained constant below the gel point and increased as the square of the gel fraction above t_g. This behavior was interpreted as a result of the interaction of the gel with the solvent. Below t_g, $S_\infty=0$ and the attenuation exhibited no changes on approach to t_g. Beyond t_g, the rise in the attenuation was interpreted as due to the increasing resistance of the water to flow around the gel. In contrast, no solvent is involved in the present epoxy system and changes in the attenuation here are seen as a direct reflection of the underlying percolation process.

To examine the frequency dependence, measurements were performed at fixed temperature for three different frequencies. In Figs. 5(a) and 5(b) the change in attenuation and decrease in transit time per unit length are shown for 2.25, 5, and 10 MHz. The attenuation has been normalized by ν^2 ($\nu=\omega/2\pi$) as it normally exhibits such a dependence. Although at short times $\Delta\alpha/\nu^2$ is roughly the same for all three frequencies, near the gel time an anomalous dispersion arises such that the normalized attenuation decreases for increasing frequency. Likewise in Fig. 5(b), the velocity exhibits dispersion effects, the velocity being larger at higher frequencies.

It is also evident that t_g (as defined by the maximum of $\Delta\alpha$) appears to exhibit a small frequency dependence and occurs earlier at higher frequency. This is in conflict with the nature of the gel point defined in PT, but may be the result of a finite-size effect. The wavelength of the pressure envelope of the acoustic wave establishes a relevant length scale and is shorter at higher frequencies. In such instances an effective percolation point can be defined whose distance from the true p_c varies as $\lambda^{-1/\nu}$ [7]. Hence, as the frequency increases the effective gel point is shifted to times earlier than the true gel point. A test of this would, however, require better precision in the determination of t_g.

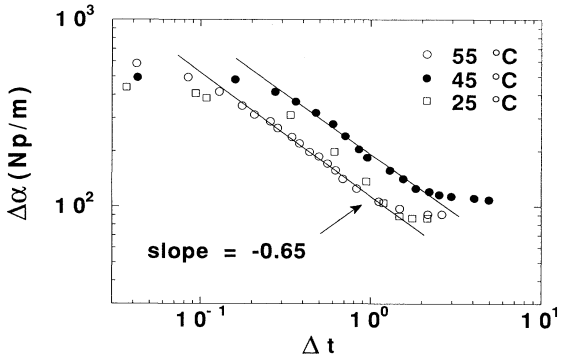

FIG. 4. Plot of $\Delta\alpha$ vs. Δt above t_g for $T=55$ °C–25 °C. The lines represent the observed power-law behavior with a slope $=-0.65\pm0.03$.

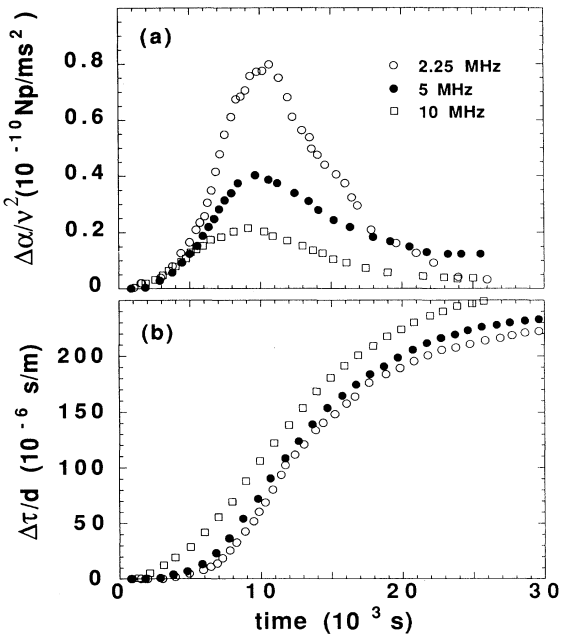

FIG. 5. (a) Change in attenuation normalized by ν^2 for $\nu=2.25$, 5, and 10 MHz. (b) Decrease in transit time per unit length for $\nu=2.25$, 5, and 10 MHz.

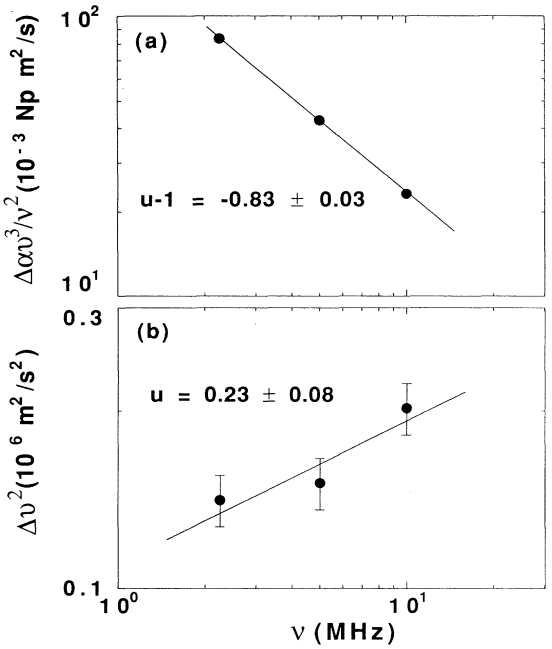

FIG. 6. (a) Plot of $\Delta\alpha v^3/\nu^2$ at $t=t_g$ vs. frequency. The line represents the fit to the power law described in the text with $u-1=-0.83\pm0.03$. (b) Plot of Δv^2 at $t=t_g$ vs. frequency. The line represents the fit to the power law described in the text with $u=0.23\pm0.08$.

To investigate the dispersion, the values of $\Delta\alpha v^3/\nu^2$ and Δv^2 at $t=t_g$ are displayed as a function of the frequency in Figs. 6(a) and 6(b), respectively. $\Delta\alpha v^3/\nu^2$ is proportional to η and thus varies according to Eq. (20a) as ω^{u-1}. From Fig. 6(a) one obtains $u-1=-0.83\pm0.03$, hence $u=0.17\pm0.03$. The power-law dispersion of Δv^2 is somewhat more difficult to interpret as the velocity changes most rapidly at $t=t_g$ and thus accrues large error. Nevertheless it is estimated that $G'=\omega^u$ with $u=0.23\pm0.08$. Thus considering both the real and imaginary parts of the shear modulus at $t=t_g$, one arrives at $u=0.20\pm0.05$. This exponent is considerably smaller than that obtained by Adam and Delsanti [11] for measurements of the complex shear modulus of branched polymers in the low-frequency range (10^{-3}–10 Hz). There they observed $u=0.70\pm0.02$, which was seen to be consistent with their measured values of k and t for the low-frequency case of ES [see Eq. (23)]. In light of the high-frequency regime studied here, a comparison with the scaling relation that results from terms in $\omega\eta$ of order ω^2 (i.e., next leading order) is deemed more appropriate. Inserting the experimentally determined values of $k_\infty=4.0\pm0.5$ and $t_\infty=0.47\pm0.03$ into Eq. (25a) and solving for the exponent u, one obtains $u=0.21\pm0.05$, in excellent agreement with the measured result.

Finally, the temperature dependence of the gelation process is considered. Measurements of the viscosity of DGEBA, performed with a Brookfield viscometer, are shown in Fig. 7, together with the temperature behavior of t_g seen at 2.25 MHz. Both display similar Arrhenius

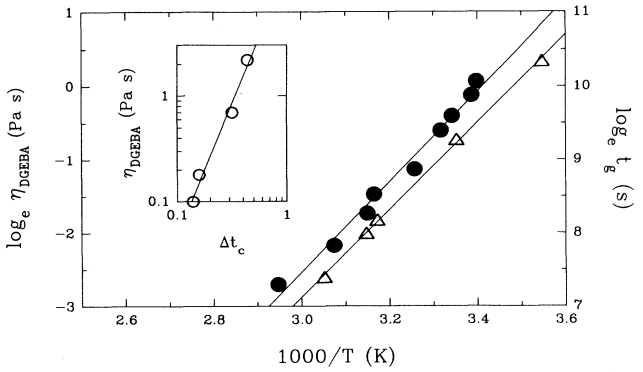

FIG. 7. Plot of the viscosity of DGEBA (closed circles) and t_g (triangles) at $\nu=2.25$ MHz vs. inverse temperature. The lines indicate the similar Arrhenius behavior observed for both. Inset: The viscosity of DGEBA vs. Δt at the crossover point. The line represents the power-law behavior described in the text with $k_0+t_\infty=2.4\pm0.3$.

behavior over the temperature range investigated and imply that t_g is mostly influenced by the initial viscosity of DGEBA, which comprises the major portion by volume of the mixture. Higher initial viscosity at colder temperature results in slower diffusion of the TETA and DGEBA and hence longer time for gelation to occur.

Returning to Fig. 2, one finds that the crossover from power-law divergence of η with exponent $k=4$ to behavior independent of Δt occurs at a specific Δt, Δt_c, which increases with decreasing temperature. From Eq. (27), this crossover at Δt_c is given by

$$\left[\frac{\omega}{G_\infty^1}\right]\eta_0^0(T)=\Delta t_c^{\,k_0+t_\infty} \quad \text{or} \quad \eta_0^0(T)\approx\Delta t_c^{\,k_0+t_\infty},$$

where G_∞^1 is assumed to vary only weakly with temperature. Furthermore, as Fig. 7 suggests that $\eta_0^0(T)$ is proportional to η of DGEBA, one finally obtains

$$\eta_{\mathrm{DGEBA}}(T)\approx\Delta t_c^{\,k_0+t_\infty}. \tag{32}$$

From Fig. 2, Δt_c has been arbitrarily taken as Δt where the extrapolation of the Δt^{-4} and Δt^0 behaviors intersect. In the inset of Fig. 7, the double logarithmic plot of η_{DGEBA} vs. Δt_c yields $k_0+t_\infty=2.4\pm0.3$. Substituting the measured values of $t_\infty=0.47\pm0.03$ and $k_0+t_\infty=2.4\pm0.3$, into the scaling relation [Eq. (24a)] one finds $u=0.20\pm0.04$, again in good agreement with the measured result.

The primary finding of this study is that the exponents k and t are significantly modified at higher frequencies. The exponent k is significantly larger than that of the static situation, while the exponent t is much lower. Furthermore, it is seen that the measured value of t is comparable to that of the gel fraction, $\beta=0.45$, and suggests that at high frequencies the elastic modulus grows in direct proportion to the growth of the infinite cluster. This implies that while in the static case dangling chains do not contribute to the shear modulus, they do contribute at higher frequencies. This is more obvious in the sit-

uation of the conductivity of a metal cluster. Although charge carriers cannot flow through a dangling chain they can oscillate within one.

It is the author's contention that the observed trends in k and t are simply a reflection of the behavior of the scaling function when ω is increased. More importantly, the specific form which these functions take depends intimately upon the limiting strategy chosen. To pursue this idea further, the scaling function which describes the behavior of the elasticity is considered in more detail.

In the limiting strategy which arose from simple viscoelasticity concepts, $\phi_+(z)$ was chosen such that a limit to infinite frequency truncates the expression leaving only the first term. This strategy differs considerably with that practiced in the scaling hypothesis approach (ES) in which a limit to zero frequency is applied. In light of the derivation presented earlier, I find no reason for preferring such a zero-frequency-limit approach. Nevertheless, consider the consequence of adopting that alternative limiting strategy. In that situation, Eq. (21) together with Eq. (22) reduce to

$$G'^{\mathrm{ES}}=G_0^1\Delta p^{t_0}\left[1+c\left[\frac{\omega}{\omega_0'}\right]\Delta p^{-k_0-t_0}+\cdots\right],$$

where t_0 is the zero-frequency limit of t. In the low-frequency limit, higher-order terms in this expression are truncated leaving the expected vanishing behavior of G'. In the high-frequency limit, however, the dominance of higher-order terms would lead to a situation in which G' *diverges* on approach to p_c. This is clearly *not observed* in the present measurements, as Δv^2 is seen to decrease as t_g is approached from above.

Further support in favor of the present limiting strategy comes from consideration of the various scaling relations which result. Equation (24b), for example, expresses the vanishing of G' in the low-frequency limit. Assuming that the measured $u=0.20\pm0.05$ is valid at low frequencies, Eq. (24b), with $t_\infty=\beta=0.45$, would yield a low-frequency elasticity that vanishes with a larger exponent, $t_0=2.9\pm0.5$. This value is consistent with the range of experimental results obtained at low frequencies including those of Adam and Delsanti, who obtained 3.2 ± 0.5. Similarly, one finds from Eq. (24a) that the low-frequency limit for k is $k_0=1.8\pm0.5$ in rough agreement with present estimates found in the literature.

One may argue that terms beyond the second term in $\phi_\pm(z)$ should also eventually dominate. It can only be assumed that there is some physical reason for which only the first-order corrections are sufficient. In any event, although the scaling relations would be altered, the limiting procedure would still result in k increasing with increasing frequency while t decreases, as has been observed. The limiting procedure chosen above indicates that it is the exponent associated with the high-frequency limit of the elasticity which is the least ambiguous. It is encouraging that the present measurements indicate that this exponent is close to that of the gel fraction β.

SUMMARY

The present work represents an attempt to interpret the results of ultrasonic measurements of a gelling epoxy resin in terms of PT. It represents also experimental evidence of what happens to PT in other than the zero-frequency limit and indicates that modest extensions of the conductivity analogy for transport properties is successful in describing the observed variations in all the measured exponents. It is observed that at higher frequency, higher-order terms contribute significantly to the transport exponents, with the result that k is generally increased, while t decreases and may even be approaching β in the limit of infinite frequency. This implies that high-frequency acoustic waves are influenced by all of the infinite cluster, including the dangling chains. If so, the present work has achieved a reduction in the number of exponents as t_∞ can now be replaced by the PT exponent β which arises solely from connectivity properties of the gel.

Both exponents (k and t) are shown to be consistent with the measured exponent that describes the dispersion at the threshold, when terms in $\omega\eta\approx\omega^2$ are retained. For the analogous case of conductivity in the metal-dielectric system, Efros and Shklovskii suggest that the ω^2 dependence is due to the dissipation of energy from isolated metal clusters. Hence the metal clusters behave roughly like oscillating antennae radiating away photons of electromagnetic energy. Possibly one could likewise envision clusters of bonded epoxy which after interacting with the incident acoustical wave (essentially an ensemble of phonons) radiate away acoustical energy in the form of phonons.

A physical mechanism for the $1/\omega$ dependence of G' at low frequency is missing at present, but may be found in the "flicker" or "$1/f$" noise that is often observed at low frequency in many amorphous systems [20].

ACKNOWLEDGMENTS

I am grateful to McMaster University for financial support and to Dr. G. P. Johari for the services of his laboratory where these measurements were performed as well as for his constructive comments on the manuscript. I also thank Dr. C. M. Sorensen for valuable discussions.

*Present address: Sandia National Laboratories, Department 1845, Albuquerque, NM 87185.

[1] P. G. de Gennes, *Scaling Concepts in Polymer Physics* (Cornell University Press, Ithaca, 1979).

[2] D. Stauffer, A. Coniglio, and M. Adam, Adv. Polym. Sci. **44**, 103 (1982).

[3] P. J. Flory, J. Am. Chem. Soc. **63**, 3083 (1941).

[4] W. H. Stockmayer, J. Chem. Phys. **11**, 45 (1943).

[5] P. G. de Gennes, J. Phys. (Paris) Lett. **37**, L1 (1976); **40**, L197 (1979).

[6] D. Stauffer, J. Chem. Soc. Faraday Trans. II **72**, 1354 (1976).

[7] D. Stauffer, *Introduction to Percolation Theory* (Taylor and Francis, London, 1987).
[8] J. E. Martin, J. Wilcoxon, and D. Adolf, Phys. Rev. A **36**, 1803 (1987).
[9] S. Arbabi and M. Sahimi, Phys. Rev. Lett. **65**, 725 (1990).
[10] D. Durand, M. Delsanti, M. Adam, and J. M. Luck, Europhys. Lett. **3**, 297 (1987).
[11] M. Adam and M. Delsanti, Contemp. Phys. **30**, 203 (1989).
[12] S. Feng, B. I. Halperin, and P. N. Sen, Phys. Rev. B **35**, 197 (1987).
[13] G. Harrison, *The Dynamic Properties of Supercooled Liquids* (Academic, London, 1976).
[14] M. Daoud, F. Family, and D. C. Hong, J. Phys. A **21**, L917 (1988).
[15] A. L. Efros and B. I. Shklovskii, Phys. Status Solidi B **76**, 475 (1976).
[16] E. K. Papadakis, J. Appl. Phys. **42**, 2990 (1971).
[17] I. Alig, M. Fedtke, K.-G. Hausler, W. Tanzer, and S. Wartewig, Prog. Colloid Polym. Sci. **78**, 54 (1988).
[18] G. P. Johari, Ann. NY Acad. Sci. **279**, 117 (1976).
[19] J.-C. Bacri, J.-M. Courdille, J. Dumas, and R. Rajaonarison, J. Phys. (Paris) Lett. **41**, L369 (1980).
[20] R. Rammal, C. Tannous, and A. M. S. Tremblay, Phys. Rev. A **31**, 2662 (1985).